

Effects of Microbus Front Structure on Pedestrian Head Injury

Xuejing Du^{1*}, Daizhong Su², Jinpeng Li³, Zhanyu Wang¹

¹ Transportation College, Northeast Forestry University, China. Emails: duxuejing99@163.com, zhanyuwang77@163.com.

² Advanced Design and Manufacturing Engineering Centre, School of Architecture, Design and the Built Environment, Nottingham Trent University, UK. E-mail: daizhong.su@ntu.ac.uk.

³ Lovol Heavy Industry Company Ltd, China. E-mail: 545553681@qq.com

*Corresponding author

Abstract: In order to study the effects of the microbus front structure on pedestrian head injury happened in pedestrian-microbus collisions, the mathematic models of the impact angle and microbus front configuration are developed, which illustrate the relationship between the impact angle, pedestrian size, and oblique angles of the engine hood and windscreen. The mathematic models are then verified by simulating experiments using LY-Dyna. The impact angle α , which is measured between the contact surface and the pedestrian head's impact direction at the contact point, is an important parameter indicating the relationship of pedestrian head injury with the microbus front structure. The analysis and simulation results reveal that (1) in the case of collision with the windscreen, the pedestrian head injury increases while α increases; (2) in the case of collision with the engine hood, the pedestrian head incurs the most serious injury when $\alpha = 90^\circ$, the pedestrian head injury increases while α increases when $\alpha < 90^\circ$, and the pedestrian head injury reduces while α increases when $\alpha > 90^\circ$. Six microbus models are taken as examples to verify the results obtained.

Key words: Vehicle engineering, Pedestrian, Microbus, Windscreen, Engine hood, Traffic injury, Head injury, Road accident

Biographical notes: Xuejing Du is an associate professor and has been working in Vehicle Engineering Department of Transportation College, Northeast Forestry University, China since 2008. She received her PhD degree in transportation engineering from Jilin University, China in 2008. Her current research involves traffic environment, vehicle collision and safety technology, and light weight design of automobile. Her research has been supported by funding from various sources including the National Natural Science Foundation of China (NSFC), Natural Science Foundation of Heilongjiang Province of China, Higher Education Funds of Heilongjiang Province of China, International Cooperation of Northeast Forestry University, Transport Research of Heilongjiang Province of China, and Fundamental Research Funds of the Central Universities. She also participated in the collaborative projects sponsored by Volkswagen and the Development and Reform Commission of Jilin Province.

Daizhong Su is Professor of Design Engineering and leads the Advanced Design and Manufacturing Engineering Centre at Nottingham Trent University, UK. His research interests include machine and mechanisms, environment protection and sustainability, integrated design and manufacturing, and condition monitoring. His research has been supported by grants from various founding organisations including European Commission, UK research funding bodies, Royal Society, industries and international organisations. He has been involved in organising more than 20 international conferences as Conference Chair, Co-chair, international chair and committee members. He has about 250 refereed publications.

Jinpeng Li is an engineer and has been working in Lovol Heavy Industry Co. Ltd since 2015. He received his master degree vehicle operation engineering from Northeast Forestry University, China in 2015. His current research involves vehicle collision and safety technology, and automotive chassis design.

Zhanyu Wang is an associate professor and has been working at the Northeast Forestry University, China since 2009. He received his PhD degree in 2009. The major areas of his research and teaching include vehicle collision and safety technology, traffic pollution and environment protection, and automobile theory/technology and simulation. His recent research is supported by the grant from the Natural Science Foundation of Heilongjiang Province, China.

1 Introduction

In pedestrian-vehicle collisions, the casualty rate of pedestrians is very high and such accidents become a serious safety problem. Pedestrians account for a high proportion of casualties in traffic accidents: 13% in the USA and 10-16% in the European Union. The injury of pedestrians takes up high proportion of traffic accident casualties, for example, amongst the traffic accident toll, 13% the deaths are pedestrians in USA (Aziz, 2013), and 10%~16% are pedestrians in European Union (Kong and Yang 2010). In developing countries, the proportion is even higher: in India, for example, it is more than 40% (Kong and Yang, 2010). In China, a pedestrian is injured in every 5 minutes and a pedestrian is killed in every 17 minutes (Xu, 2009). Therefore, protecting pedestrians from traffic accidents is an important issue which draws great attention worldwide, and consequently many pedestrian protection methods have been proposed/developed, such as the air bag system (Song, 2009) and the integrated electronic security system (Chu, 2008). Extensive research has also been conducted on the effects of pedestrian-vehicle collisions on the human body (Cheol, 2008 and Cui, 2009).

In traffic accidents, various factors affect the position and severity of the pedestrians' injuries, including their height and physical condition, the contact angle with the vehicle, their physical surroundings, and the size, structure and speed of vehicle. According to the literature, in pedestrian-vehicle collisions, the part of the human body with the highest frequency of injury is the pedestrian's head, which often leads to permanent disability or death (Fredriksson, 2012 and HAN, 2012). Therefore, reducing head injuries in traffic accidents has drawn great attention worldwide. In Germany and Japan, the prevention of head injury from traffic accidents is a specific research topic in the study of human body injury (Ehrlich, 2009 and Maki, 2003). Elliott (2012) studied how the pedestrian's head injury was affected by their own speed and style of movement, as well as the vehicle's speed. Based on the simulation of pedestrian-vehicle collision, Yao (2008) pointed out that in some areas of windscreen, particularly in its areas with high intensity or strength, the pedestrian head protection appliance should be installed.

Researchers have conducted investigations on pedestrian's head injury in pedestrian-vehicle collision, such as the effect of impact velocity on the pedestrian's head injury, and the impact of the pedestrian's head with the windscreen and engine hood (Peng, 2012 and Qiao, 2006). Crocetta, et al. (2015) investigated the influence of, Sport Utility Vehicle and Van front height and shape in pedestrian accidents on the mechanism of impact with the ground and on head-ground impact speed.

However, the existing studies rarely involve microbus, and little has been done on the effect of vehicle's front structure in relation to pedestrian's head injury. In some countries, such as China, minibuses have been widely used due to their characteristics of low economic cost and bigger capacity in comparison with cars; however, they have a high accident rate and disastrous personnel casualty in traffic accidents.

To address the issues mentioned above, the research presented in this paper investigates the influence of microbus front structure on the head injury of pedestrians, and, based on the investigation results, to optimize the microbus front structure, including the engine hood and windscreen, in order to reduce the head injury of pedestrians involved in traffic accidents related to minibuses.

2 Equations of collision and pedestrian head injury

2.1 Contact collision equations

Explicit algorithm is applied in LS-Dyna, which is suitable for nonlinear structural impact dynamics. Central difference time integral method is used to calculate instantaneous accelerator of each node of the dynamic system. The instantaneous accelerator $\mathbf{a}(t_n)$ is given as equation (1).

$$\mathbf{a}(t_n) = \mathbf{M}^{-1} [\mathbf{P}(t_n) - \mathbf{F}^{\text{int}}(t_n)] \quad (1)$$

Where, \mathbf{M} is the mass matrix, \mathbf{P} is the external force vector, and \mathbf{F}^{int} is the internal force vector.

The internal force \mathbf{F}^{int} can be calculated by equation (2).

$$\mathbf{F}^{\text{int}} = \int_{\Omega} \mathbf{B}^T \boldsymbol{\sigma} d\Omega + \mathbf{F}^{\text{hg}} + \mathbf{F}^{\text{contact}} \quad (2)$$

Where, $\int_{\Omega} \mathbf{B}^T \boldsymbol{\sigma} d\Omega$ is equivalent node force of a unit stress field, \mathbf{F}^{hg} is hourglass resistance force, and $\mathbf{F}^{\text{contact}}$ is contact force.

The speed vector and displacement vector of the node are given by equation (3) and equation (4) respectively.

$$\mathbf{v}(t_{n+1/2}) = \mathbf{v}(t_{n-1/2}) + 0.5\mathbf{a}(t_n)(\Delta t_{n-1} + \Delta t_n) \quad (3)$$

Where, $\mathbf{v}(t_{n+1/2})$ is speed vector of the node at time $t_{(n+1/2)}$, $\mathbf{v}(t_{n-1/2})$ is speed vector of the node at time $t_{(n-1/2)}$, the instantaneous accelerator $\mathbf{a}(t_n)$ given by the above equation (1), and Δt_n is the time increment.

$$\mathbf{u}(t_{n+1}) = \mathbf{u}(t_n) + \mathbf{v}(t_{n+1/2})\Delta t_n \quad (4)$$

Where, $\mathbf{u}(t_{n+1})$ is displacement vector of the node at time $t_{(n+1)}$, $\mathbf{u}(t_n)$ is the displacement vector of the node at time t_n , $\mathbf{v}(t_{n+1/2})$ is the speed vector of the node at time $t_{(n+1/2)}$, and Δt_n is the time increment.

The time increments Δt_{n-1} and Δt_n , and time points $t_{n-1/2}$ and $t_{n+1/2}$ can be calculated by equation (5) and equation (6) respectively:

$$\Delta t_{n-1} = t_n - t_{n-1}, \quad \Delta t_n = t_{n+1} - t_n \quad (5)$$

$$t_{n-1/2} = 0.5(t_n + t_{n-1}), \quad t_{n+1/2} = 0.5(t_n + t_{n+1}) \quad (6)$$

The new geometric configuration can be obtained by adding the displacement increment to the initial configuration, as shown in Equation (7).

$$\mathbf{x}_{t+\Delta t} = \mathbf{x}_0 + \mathbf{u}_{t+\Delta t} \quad (7)$$

Where, $\mathbf{x}_{t+\Delta t}$ is the new geometric configuration, \mathbf{x}_0 is the initial configuration, and $\mathbf{u}_{t+\Delta t}$ is the displacement increment.

To meet the stability condition of explicit algorithm and to ensure the convergence, the boundary time increment must meet the following

$$\Delta t \leq \frac{2}{\omega_n} \quad (8)$$

Where, ω_n is the highest order natural frequency of the system.

2.2 Pedestrian head injury equation

Equation (9) is the formula of Head Injury Criteria (*HIC*), which is the key assessment index of pedestrian head injury (Liu Kaiyang, 2009). *HIC*=1000 is the safety limit of head injury in a pedestrian-vehicle collision with speed 50km/h, according to GB11551-2003 (Xu, 2014).

$$HIC = \max_{t_1 < t_2, t_2 - t_1 \leq 15\text{ms}} \left\{ \left[\frac{1}{t_2 - t_1} \int_{t_1}^{t_2} a(t) dt \right]^{2.5} (t_2 - t_1) \right\} \quad (9)$$

where, $a(t)$ is resultant acceleration of the pedestrian head, t_1 is start time. t_2 is end time.

3 Mathematic models

3.1 Basics of the modelling

Figure 1 is the impact schematic diagram of pedestrian head colliding with microbus. When pedestrian collides with microbus, pedestrian rotates around point A of the microbus, and the pedestrian head could collide with the engine hood or windscreen with an angle subject to the support of human skeleton.

In the process of the pedestrian colliding with the microbus, the impact angle α between impact direction of the pedestrian head and the engine hood or windscreen is determined by the frontal structure and configuration of the microbus and the pedestrian height.

When a pedestrian collides with the engine hood or windscreen, Head Injury Criteria (*HIC*) of the pedestrian

head can be calculated by equation (10), which is derived by introducing impact angle α , as shown in Figure 1, into equation (9).

$$HIC = \max_{t_1 < t_2, t_2 - t_1 \leq 15ms} \left\{ [\sin \alpha]^{2.5} \left[\frac{1}{t_2 - t_1} \int_{t_1}^{t_2} a(t) dt \right]^{2.5} (t_2 - t_1) \right\} \quad (10)$$

where, α is the impact angle that the pedestrian's head collides with the microbus's engine hood or windscreen, which is measured between the contact surface and the impact direction of the pedestrian head at the contact point, as shown in Figure 1.

Figure.1 Pedestrian head colliding with microbus

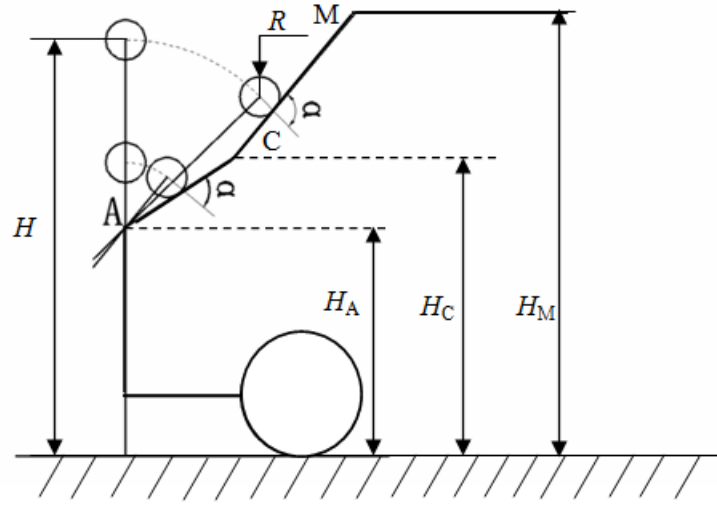
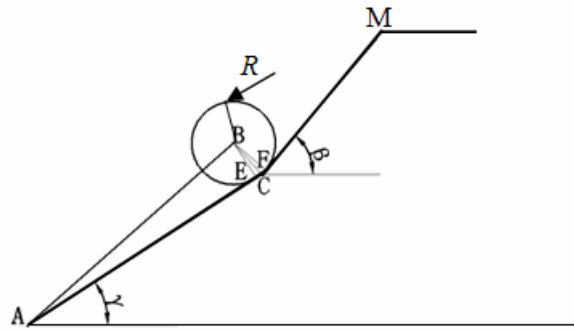


Figure 2 shows the situation that pedestrian's head collides with microbus at the joint between the engine hood and the windscreen. In such a case, as shown in Figure.2, $BE \perp AC$, $BF \perp CF$, $BE = BF = R$, then, equation (11) and equation (12) can be obtained.

Figure.2 Pedestrian head colliding with microbus's engine hood and windscreen simultaneously



$$\angle BCE = \angle BCF = 90^\circ - \frac{\beta - \gamma}{2} \quad (11)$$

$$EC = BE \cot \angle BCE = R \cot \left(90^\circ - \frac{\beta - \gamma}{2} \right) \quad (12)$$

According to equation (12), equation (13) is given as follows

$$AB = \sqrt{AE^2 + BE^2} = \sqrt{(AC - EC)^2 + R^2} = \sqrt{\left[AC - R \cot \left(90^\circ - \frac{\beta - \gamma}{2} \right) \right]^2 + R^2} \quad (13)$$

Thus, when the pedestrian head's simultaneously collides with the engine hood and windscreen, the height of pedestrian is defined as H_0 , which can be calculated by equation (14).

$$H_0 = H_A + AB + R = H_A + R + \sqrt{\left[AC - R \cot\left(90^\circ - \frac{\beta - \gamma}{2}\right)\right]^2 + R^2} \quad (14)$$

Where, H_A is the leading edge's height of the microbus engine hood, R is the radius of the pedestrian head, AC is the length of the microbus engine hood, β is the angle between windscreen and horizontal direction, and γ is the angle between engine hood and horizontal direction.

3.2 Mathematic model of the pedestrian's head colliding with engine hood

When the pedestrian height meets $H < H_0$, the pedestrian rotates around point A of the microbus and collides with microbus's engine hood, as shown in Figures 3 and 4.

Figure.3 pedestrian head colliding with microbus's engine hood

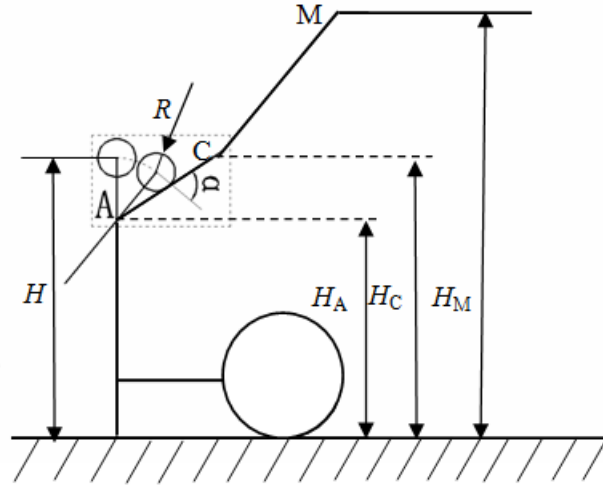
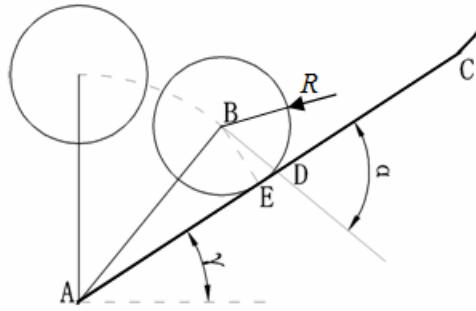


Figure.4 partial enlarged of pedestrian head colliding with microbus's engine hood



In Figure.4, $BE \perp AD$, $AB \perp BD$, $BE = R$. α is angle between impact direction of head and engine hood, And γ is the angle between engine hood and horizontal direction. Triangle ABE can be calculated by equation (15).

$$\angle BAE = \arcsin \frac{BE}{AB} = \arcsin \frac{R}{H - H_A - R} \quad (15)$$

Where, H is the pedestrian's height. Equation (16) is the impact angle's formula that pedestrian's head collides with microbus's engine hood based on equation (15).

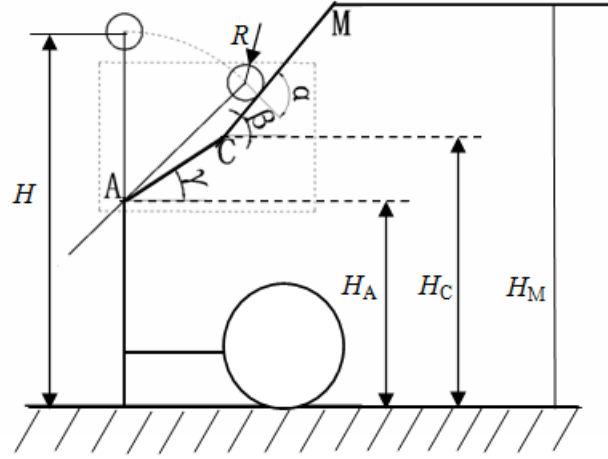
$$\angle BDA = \angle \alpha = 90^\circ - \angle BAE = 90^\circ - \arcsin \frac{R}{H - H_A - R} \quad (16)$$

According to equation (16), when pedestrian's head collides with microbus's engine hood with a impact angle less than 90° , the impact angle is affected by the pedestrian's height H , the head's radius R and the leading edge's height of engine hood H_A . With the increasing of the height of the engine hood leading edge, the impact angle α decreases. Based on equation (10), when the impact angle $\alpha < 90^\circ$, with the impact angle decreasing, the pedestrian's head injury eases. Therefore, increasing the height of engine hood leading edge can decrease the collision angle and reduce the head injury of the pedestrian.

3.3 Mathematic model of pedestrian's head colliding with the windscreen

When the height of pedestrian meets $H > H_0$, the pedestrian rotates around point A of the microbus and collides with microbus's windscreen. Figure.5 shows the pedestrian collide with microbus's windscreen. α is the angle between the impact direction of the head and engine hood. β is the angle between windscreen and horizontal direction. γ is the angle between the engine hood and horizontal direction. Figure.6 is the partially enlarged sketch drawing of pedestrian's head collide with microbus's windscreen.

Figure.5 Pedestrian collides with microbus's windscreen



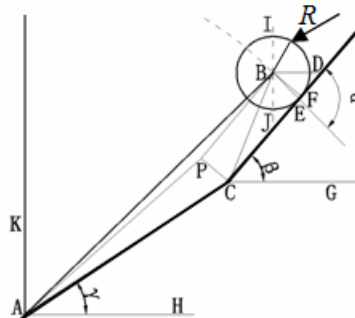
In Figure.5, angle β and angle γ can be calculated by equation (17) and equation (18) respectively.

$$\angle \beta = \arcsin \frac{H_M - H_C}{CM} \quad (17)$$

$$\angle \gamma = \arcsin \frac{H_C - H_A}{AC} \quad (18)$$

Where, H_M is the height of the windscreen upper edge, H_C is the height of the windscreen lower edge or the height of the engine hood trailing edge, H_A is the leading edge's height of the engine hood, AC is the length of the engine hood, CM is the length of the windscreen, β is the angle between windscreen and horizontal direction, and γ is the angle between the engine hood and horizontal direction.

Figure.6 Partial enlarged of pedestrian head collide with microbus's windscreen



As shown in Figure.6, $BD \parallel CG \parallel AH$, $BF \parallel PC$, $AK \perp AH$, $AB \perp BE$, $BF \perp CF$, $IJ \perp BD$, $BF=PC=R$, and BE is the impact direction. In Figure.6, angle α can be calculated by equations (19), (20) and (21).

$$\angle ABJ + \angle JBE = \angle KAB + \angle JBE = \angle DBE + \angle JBE = 90^\circ \quad (19)$$

$$\angle KAB = \angle DBE \quad (20)$$

$$\angle \alpha = \angle BEC = \angle DBE + \angle BDE = \angle KAB + \angle \beta = 90^\circ - \angle BAC - \angle \gamma + \angle \beta \quad (21)$$

According to the relationship of inside angles and edges, triangle ABC and edge AB can be obtained by equation (22) and equation (23)

$$\angle BAC = \arccos \frac{AB^2 + AC^2 - BC^2}{2 \times AB \times AC} = \arccos \frac{AB^2 + AC^2 - (BF^2 + FC^2)}{2 \times AB \times AC} \quad (22)$$

$$AB = H - H_A - R \quad (23)$$

Equation (24) is the formula of impact angle α between impact direction and microbus's windscreen based on equations (21), (22) and (23).

$$\angle \alpha = 90^\circ + \angle \beta - \angle \gamma - \arccos \frac{(H - H_A - R)^2 + AC^2 - R^2 - FC^2}{2 \times (H - H_A - R) \times AC} \quad (24)$$

According to the relationship of the inside angles and edges in triangle APC , equations (25-27) can be obtained.

$$\angle ACP = 90^\circ + \angle \gamma - \angle \beta \quad (25)$$

$$AP = \sqrt{AC^2 + PC^2 - 2AC \times PC \cos \angle ACP} = \sqrt{AC^2 + R^2 - 2AC \times R \cos(90^\circ + \angle \gamma - \angle \beta)} \quad (26)$$

$$\angle APC = \arcsin \left(\frac{AC}{AP} \sin \angle ACP \right) = \arcsin \left[\frac{AC}{AP} \sin(90^\circ + \angle \gamma - \angle \beta) \right] \quad (27)$$

According to the relationship of inside angles and edges in triangle ABP , equations (28-29) can be obtained.

$$\angle APB = 270^\circ - \angle APC = 270^\circ - \arcsin \left[\frac{AC}{AP} \sin(90^\circ + \angle \gamma - \angle \beta) \right] \quad (28)$$

$$\cos \angle APB = \frac{AP^2 + BP^2 - AB^2}{2 \times AP \times BP} = \frac{AP^2 + FC^2 - AB^2}{2 \times AP \times FC} \quad (29)$$

According to equation (29), FC can be calculated by equation (30).

$$FC = AP \cos \angle APB + \sqrt{AB^2 - AP^2 \sin^2 \angle APB} \quad (30)$$

Equation (31) is the formula of impact angle α between the impact direction and microbus's windscreen based on equations (17), (18), (24), (26), (28) and (30).

$$\begin{cases} \angle \alpha = 90^\circ + \angle \beta - \angle \gamma - \arccos \frac{(H - H_A - R)^2 + AC^2 - R^2 - FC^2}{2 \times (H - H_A - R) \times AC} \\ \angle \beta = \arcsin \frac{H_M - H_C}{CM} \\ \angle \gamma = \arcsin \frac{H_C - H_A}{AC} \\ FC = AP \cos \angle APB + \sqrt{AB^2 - AP^2 \sin^2 \angle APB} \\ AP = \sqrt{AC^2 + R^2 - 2AC \times R \cos(90^\circ + \angle \gamma - \angle \beta)} \\ \angle APB = 270^\circ - \arcsin \left[\frac{AC}{AP} \sin(90^\circ + \angle \gamma - \angle \beta) \right] \end{cases} \quad (31)$$

According to equation (31), when pedestrian's head collides with the windscreen, impact angle α is affected by a set of collision parameters including the pedestrian's height H , the head's radius R , the height of the engine

hood leading edge H_A , the height of the windscreen lower edge or the height of the engine hood trailing edge H_C , the height of windscreen upper edge H_M , the length of engine hood AC and the length of windscreen CM . Because impact angle α directly affects the pedestrian head injury, any change of the collision parameters affects the pedestrian head injury.

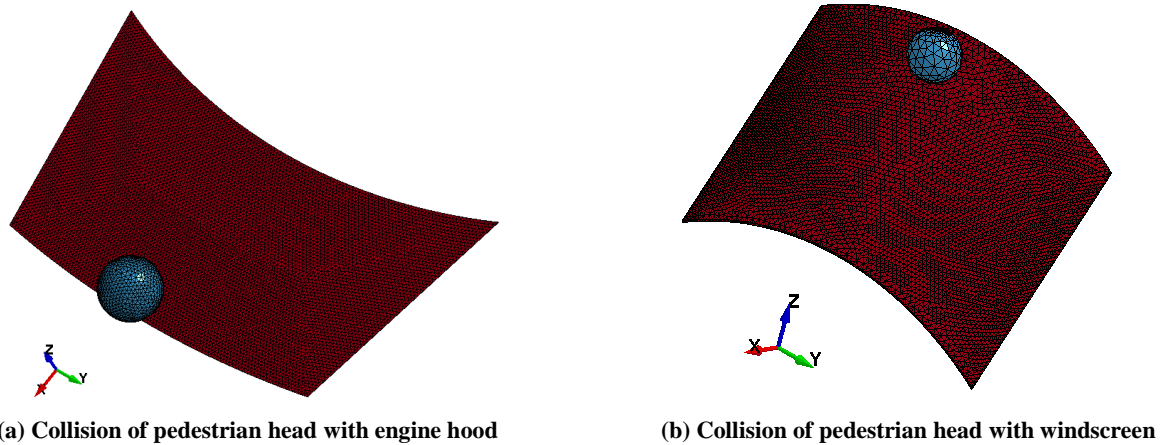
4 Simulation verification

4.1 Simulation models

In order to verify the mathematic modeling and discussion presented above, the computer simulation is conducted. The three-dimensional models of microbus's windscreen, engine hood and pedestrian head are built using CAD software Unigraphics (UG) first, and then the CAD models are imported into ANSYS to create finite element analysis (FEA) models. With the FEA models created, the collision simulation is conducted in LS-Dyna.

Within the simulation modelling, the following data are used: the microbus's windscreen is made of laminated glass, and its thickness is 5.76mm; the engine hood is made of steel material, and its thickness is 0.8mm; according to the test method designated by working group WG17 of the European Enhanced Vehicle-safety Committee (EEVC), the pedestrian head's diameter is 165mm and the head's weight is 4.8kg. The pedestrian's head is simplified into a sphere. Figure 7 are simulation models of pedestrian head colliding with the microbus engine hood and windscreen.

Figure.7 Simulation models



(a) Collision of pedestrian head with engine hood

(b) Collision of pedestrian head with windscreen

In the simulation tests with ANSYS/LS-Dyna, the collision initial velocity is 13.5m.s^{-1} , the impact angle varies from 30° to 150° for the collision of the pedestrian head with the windscreen, and the impact angle varies from 30° to 90° for the collision of pedestrian head with the engine hood.

A visco-elastic material model is adopted for the microbus windscreen. Equation (32) is the formula of the model's deviator features.

$$\sigma_{ij} = 2 \int \phi(t - \tau) \left[\frac{\partial \varepsilon'_{ij}(\tau)}{\partial \tau} \right] d\tau \quad (32)$$

Where, $\phi(t)$ is the shear slack variable which can be calculated from equation (33) below.

$$\phi(t) = G_\infty + (G_0 - G_\infty)e^{-\beta t} \quad (33)$$

Where, G_0 is the shear mod-origin, G_∞ is the shear mod-infinity, and $1/\beta$ is the attenuation coefficient.

The kinematics plastic material model, a mixture model of isotropic and kinematics hardening, is used for modelling the engine hood and pedestrian head in LS-Dyna. Failure can be considered in this model, which is associated with a strain rate. The strain rate of this model is Cowper-Symonds. Equation (34) is used to calculate yield stress which is expressed by factors related to the strain rate.

$$\sigma_Y = \left[1 + \left(\frac{\varepsilon}{C} \right)^{\frac{1}{P}} \right] (\sigma_0 + \beta E_P \varepsilon_P^{eff}) \quad (34)$$

Where, σ_Y is yield stress, σ_0 is initial yield stress, ε is strain rate, C is the strain rate parameter, ε_P^{eff} is effective plastic strain, and E_P is plastic hardening modulus.

The material data of the microbus windscreen, engine hood and pedestrian head are shown in table1.

Table.1 Material parameters of the simulation model

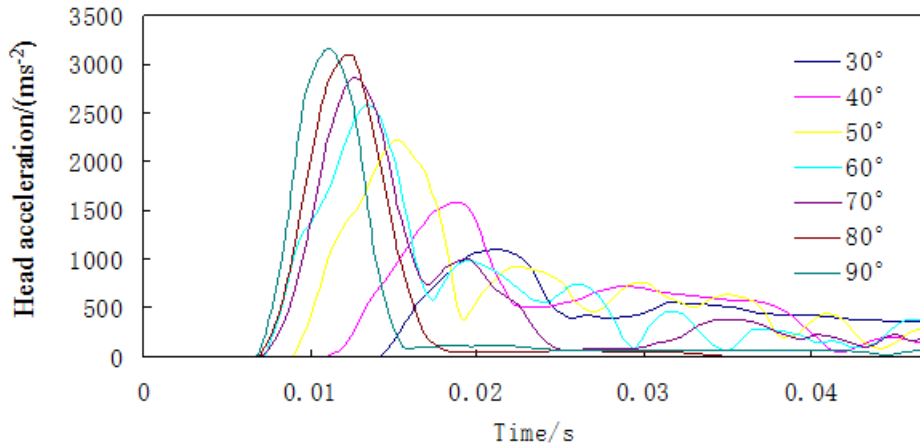
	Density ($\text{kg}\cdot\text{m}^{-3}$)	Elasticity Modulus (Pa)	Poisson Ratio	Yield strength (MPa)	Failure Strain	Shear Mod-Origin G_0 (MPa)	Shear Mod-Infinity G_∞ (MPa)	Reciprocal of Beta Y_β
Head	2040	15e9	0.21	90	0.015	-	-	-
Engine hood	7850	210e9	0.30	355	0.24	-	-	-
Windshield	2500	37e9	-	-	-	110	23	1.5

4.2 Results analysis

4.2.1 Analysis of the pedestrian head's collision with the engine hood

In order to calculate the HIC of the pedestrian head's collision with the microbus engine hood, the pedestrian head's acceleration at different times during the collision is required. In this research, the head acceleration varying with time during the collision is obtained from the collision simulation in LS-Dyna. Figure 8 is the head acceleration time history curve during the collision with impact angles 30° , 40° , 50° , 60° , 70° , 80° and 90° .

Figure 8 Head acceleration time history curve (collision of pedestrian head with engine hood)



The pedestrian head's maximum acceleration A_{\max} during the collision with the engine hood can be found from Figure 8. The values of A_{\max} are then inputted into equation (10) to calculate the HIC in corresponding to impact angle α . The values of HIC , A_{\max} and related impact angle α for the pedestrian head's collision with the engine hood are shown in Table 2.

Table.2 Simulation results of pedestrian head colliding with engine hood

α	30°	40°	50°	60°	70°	80°	90°
A_{\max}	1101.2	1588.8	2224.8	2579.9	2869.6	3083.5	3156.1
HIC	645.6	1266	2885	3711	4684	5343	5574

Figure 9 shows the relationships between impact angle α with A_{\max} and HIC based on the data shown in Table 2. As results shown in Table 2 and Figure 9, with the increase of impact angle α , the maximum acceleration A_{\max} and HIC 's values increase.

Figure.9 Relationship of impact α with A_{max} and HIC (pedestrian head colliding with engine hood)

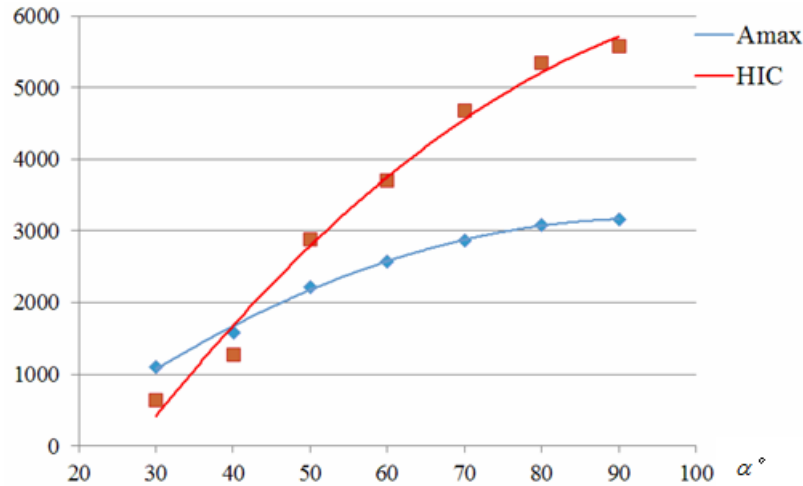
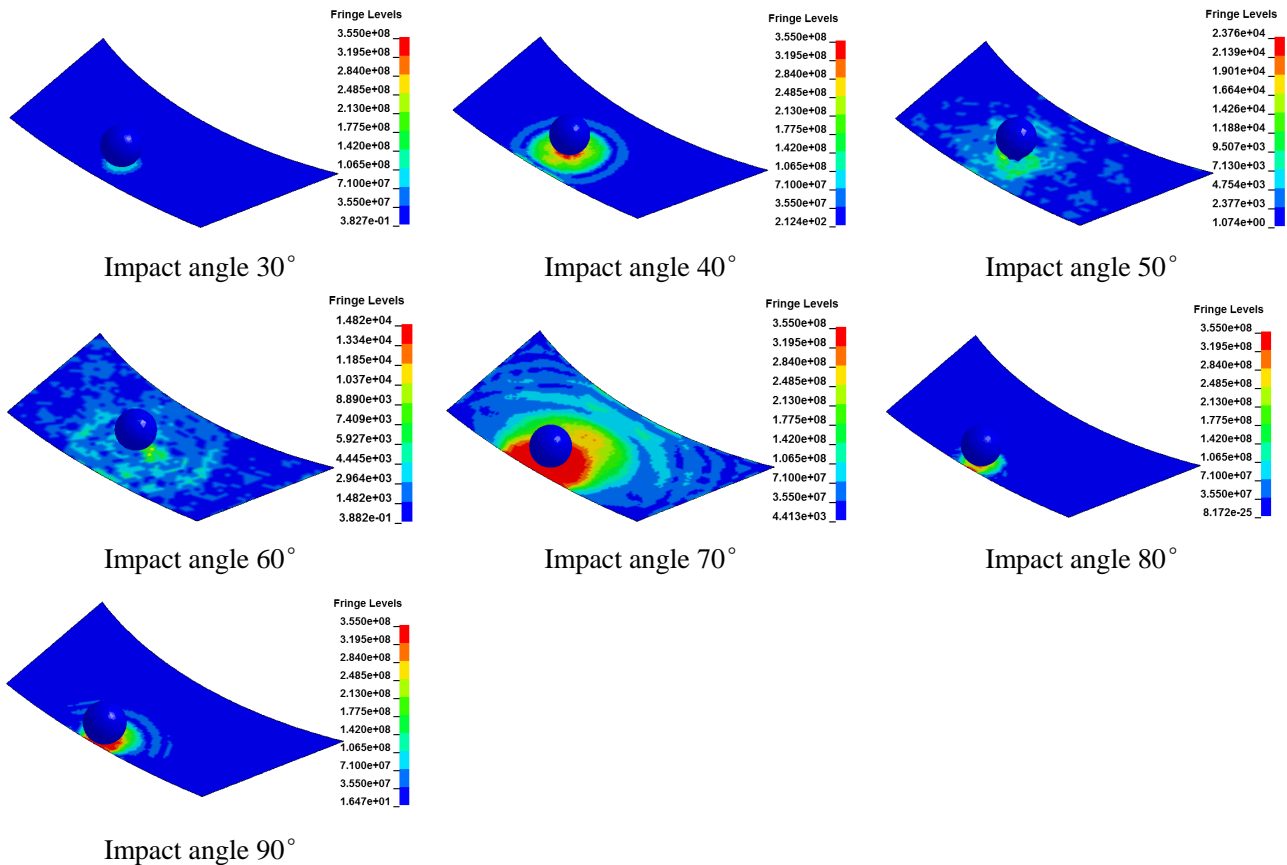


Figure 10 shows the stresses of the microbus engine hood and the pedestrian head during their collision at impact angles 30° , 40° , 50° , 60° , 70° , 80° and 90° respectively. The stresses are obtained from the collision simulation conducted in LS-Dyna.

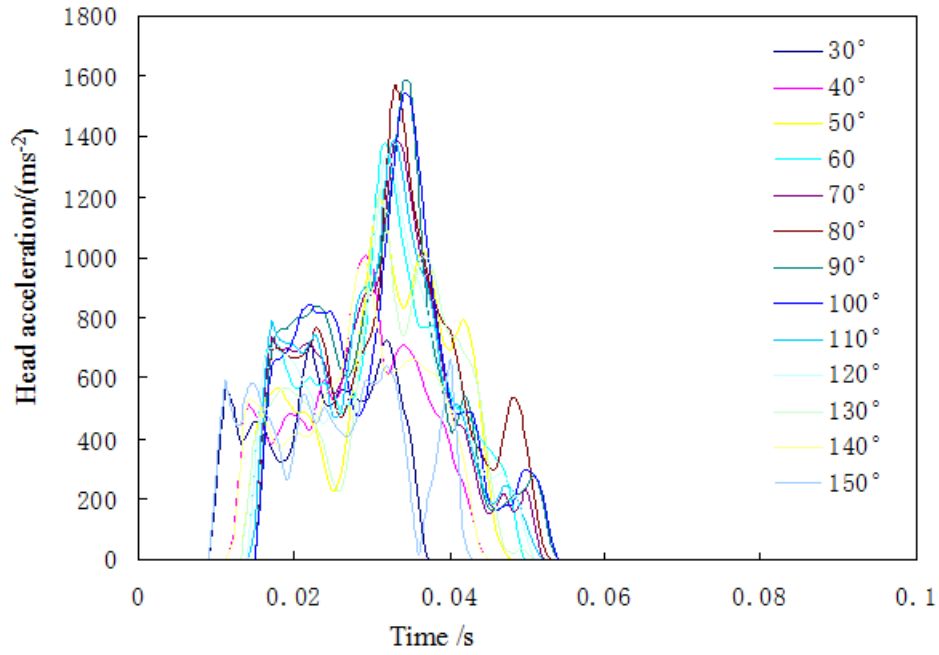
Figure10 Stresses of the microbus engine hood and pedestrian head during their collision



4.2.2 Analysis of the pedestrian head's collision with the windscreen

When the pedestrian head collides with the microbus's windscreen in different impact angles, the head acceleration varies with time during the collision. In this research, the values of the pedestrian head's acceleration are obtained from the simulation conducted in LS-Dyna. Figure 11 is the head acceleration time history curve during the collision with different impact angles.

Figure 11 Head acceleration time history curve (Pedestrian collides with windscreen)



The pedestrian head's maximum acceleration A_{\max} during the collision with the microbus' windscreen can be found from Figure 11. The values of A_{\max} are then inputted into equation (10) to calculate the HIC in corresponding to impact angle α . The values of HIC , A_{\max} and related impact angle α for the pedestrian head's collision with the windscreen are shown in Table 3.

Table.3 Simulation results of pedestrian head colliding with windshield

α	30°	40°	50°	60°	70°	80°	90°	100°	110°	120°	130°	140°	150°
$A_{\max} / (10^{-4} \text{m.s}^{-2})$	731.2	1004.2	1213.4	1378	1384.2	1560.9	1582	1535.8	1386.9	1345.8	1222.3	983.9	663.27
HIC	398.7	638.2	1198	1053	1294	1377	1485	1339	1260	1108	1118	636.2	276

Figure.12 Relationship of impact α with A_{\max} and HIC (colliding with windscreen)

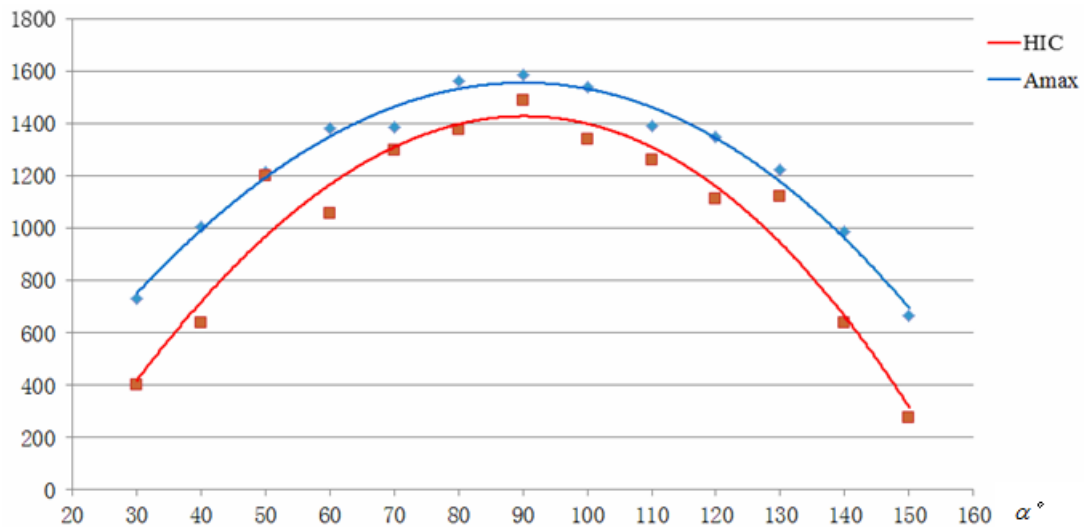
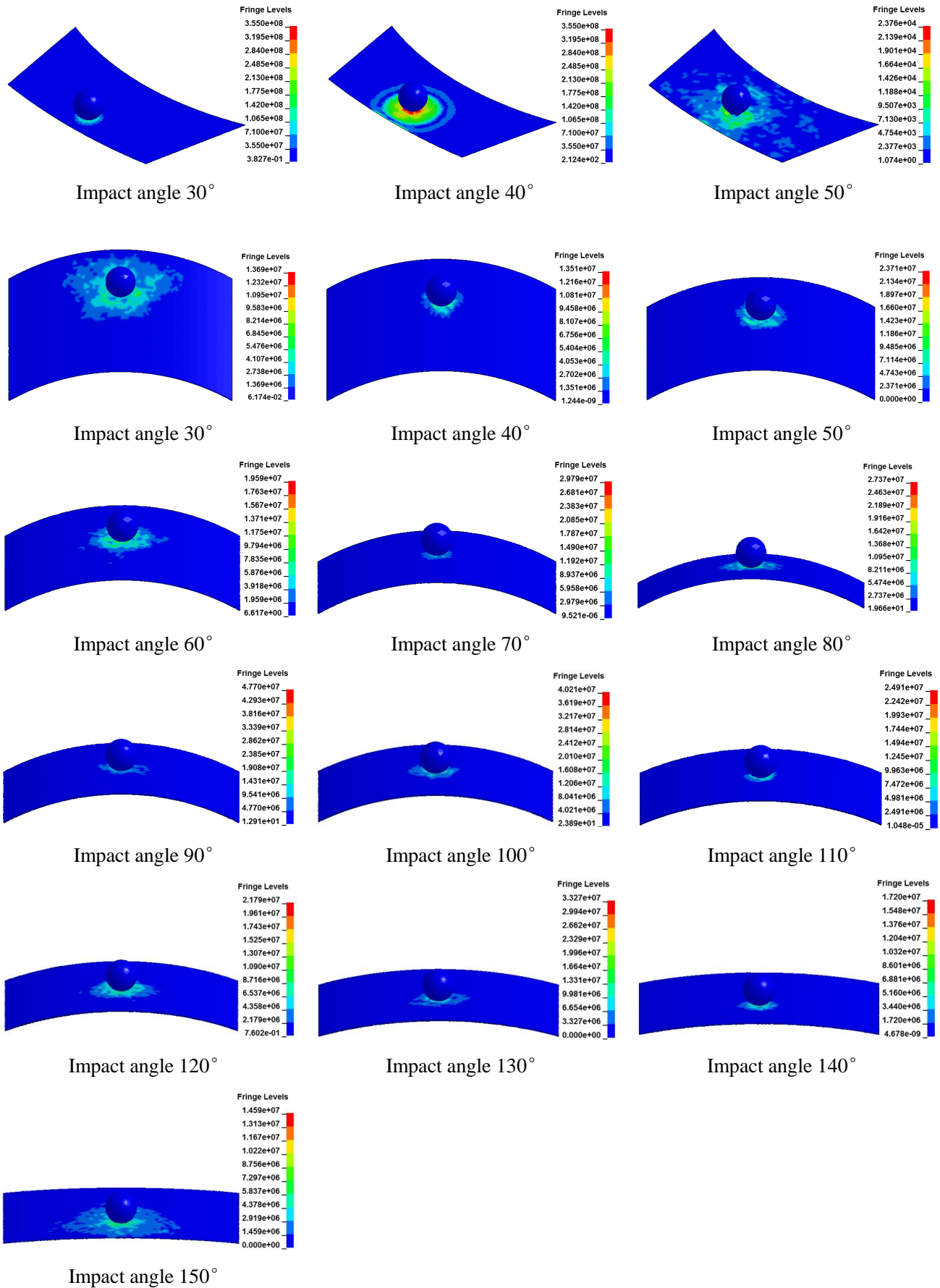


Figure 13 Stresses of the microbus windscreen and pedestrian head during their collision



The relationship of impact α with A_{\max} and HIC is further illustrated in Figure 12: when the impact angle $\alpha < 90^\circ$, with the impact angle's increasing, the maximum acceleration A_{\max} and HIC 's values increase, indicating that the degree of the pedestrian's head injury increases. When the impact angle $\alpha > 90^\circ$, with the impact angle's increasing, the maximum acceleration A_{\max} and HIC 's values decrease, indicating that the degree of the pedestrian's head injury decreases. When the impact angle $\alpha = 90^\circ$, the maximum acceleration A_{\max} and HIC 's values are the largest and the pedestrian's head injury is the most serious.

Figure 13 shows the stresses of the microbus windscreen and the pedestrian head during their collision at impact angles 30° , 40° , 50° , 60° , 70° , 80° , 90° , 100° , 110° , 120° , 130° , 140° and 150° respectively. The stresses are obtained from the collision simulation conducted in LS-Dyna.

4.2.3 Relationship between the impact angle α and the microbus' front structure parameters

According to the analyses of the pedestrian head's collisions with the windscreen and engine hood of the microbus presented in the above sections, it can be seen that the impact angle α is directly related to the pedestrian head injury. Therefore, in order to investigate the microbus' front structure's effect on the pedestrian's head injury, it is necessary to investigate the relationship between the impact angle α and the microbus' front structure parameters. The microbus front structure parameters to be investigated include the leading edge's height of microbus engine hood H_A , the height of windscreen lower edge (or the height of engine hood trailing edge) H_C , the height of windscreen upper edge H_M , the length of engine hood AC and the length of windscreen CM .

Keeping the pedestrian's height and head radius unchanged while changing the microbus front structure parameters, the corresponding values of the impact angle α can be obtained from equation (16) and equation (31), are shown in table 4.

According to the data sets of No.1~No.3 in Table 4, with the leading edge's height of microbus engine hood H_A 's increasing from 950mm to 1150mm, the impact angle α reduces 7.8° . Therefore, when pedestrian's head collides with microbus's engine hood, with the increase of the leading edge's height of microbus engine hood H_A , the impact angle α decreases and the degree of head's injury reduces.

Table.4 Impact angle changes with H_A , H_C , H_M , AC and CM

No.	H (mm)	H_A (mm)	H_C (mm)	H_M (mm)	AC (mm)	CM (mm)	α
1	1500	950	1250	1850	550	800	79.84°
2	1500	1050	1250	1850	550	800	77.03°
3	1500	1150	1250	1850	550	800	72.04°
4	1750	1050	1250	1850	550	800	105.93°
5	1750	950	1250	1850	550	800	95.18°
6	1750	850	1250	1850	550	800	85.51°
7	1750	950	1350	1850	550	800	77.21°
8	1750	950	1250	1850	550	800	95.18°
9	1750	950	1150	1850	550	800	112.02°
10	1750	950	1250	1950	550	800	104.17°
11	1750	950	1250	1850	550	800	95.18°
12	1750	950	1250	1750	550	800	87.72°
13	1750	950	1250	1850	650	800	102.19°
14	1750	950	1250	1850	550	800	95.18°
15	1750	950	1250	1850	450	800	87.65°
16	1750	950	1250	1850	550	900	90.10°
17	1750	950	1250	1850	550	800	95.18°
18	1750	950	1250	1850	550	700	102.73°

According to the data sets of No.4~No.6 in Table 4, with the leading edge's height of microbus engine hood H_A increasing from 850mm to 1050mm, the impact angle α increases 20.42°. Therefore when the pedestrian's head collides with microbus's windscreen, with the leading edge's height of microbus engine hood H_A increasing, the impact angle α increases.

According to No.7~No.9 in Table 4, with the height of windscreen lower edge (or the height of engine hood trailing edge) H_C increasing from 1150mm to 1350mm, the impact angle α reduces 34.81°. Therefore when pedestrian's head collides with microbus' windscreen, with the height of windscreen lower edge (or the height of engine hood trailing edge) H_C increasing, the impact angle α decreases.

According to the data sets of No.10~No.12 in Table 4, with the height of windscreen upper edge H_M increasing from 1750mm to 1950mm, the impact angle α increases 16.45°. Therefore when pedestrian's head collides with microbus's windscreen, with the height of windshield upper edge H_M increasing, the impact angle α increases.

According to the data sets of No.13~No.15 in Table 4, with the length of microbus's engine hood AC increasing from 450mm to 650mm, the impact angle α increases 14.54°. Therefore, when pedestrian head collides with microbus's windscreen, with the length of microbus's engine hood AC increasing, the impact angle α increases.

According to the data sets of No.16~No.18 in Table 4, with the length of windscreen CM increasing from 700mm to 900mm, the impact angle α reduces 12.63°. Therefore, when pedestrian's head collides with microbus's windscreen, with the length of windshield CM increasing, the impact angle α decreases.

As mentioned above, when pedestrian's head collides with microbus's windscreen, with the leading edge's height of microbus engine hood H_A , the height of windscreen upper edge H_M , and the length of microbus's engine hood AC increasing, the impact angle α increases; with the height of windscreen lower edge (or the height of engine hood trailing edge) H_C and the length of windscreen CM increasing, the impact angle α decreases.

4.3 Case study

According to the statistics (GB/T10000-88,1988), the range from 1449mm to 1814mm is defined as adults' height in China. Six microbus models of four microbus manufacturers are taken as samples in this research, the impact angles α_1 between impact direction of pedestrian's head and windscreen calculated by equation (31), and the impact angles α_2 between impact direction of pedestrian's head and engine hood calculated by equation (16) are both shown in Table 5. It can be seen from Table 5, when pedestrian collides with microbus's windscreen, the impact angle α_1 range from 80° to 101°, the pedestrian's head injury $HIC>1500$, hence, the pedestrian suffers from serious head injury. Therefore, it is proposed to modify the microbus front structure to reduce the head injury.

Taking microbus Changan Star as an example, its current impact angle α_1 between impact direction of head and windscreen ranges from 81.24° to 85.15°, and hence the head injury of pedestrian could be reduced by decreasing the leading edge's height of microbus engine hood H_A , the height of windshield upper edge H_M , and the length of engine hood AC , or by increasing the height of windshield lower edge (or the height of engine hood trailing edge) H_C and the length of windshield CM .

Table.5 Impact angles of different vehicle models

Models	H_A (mm)	H_C (mm)	H_M (mm)	AC (mm)	CM (mm)	α_1	α_2
Wuling Rongguang	950	1150	1850	450	950	95.83° ~ 100.33°	78.58° ~ 79.25°
Wuling Sunshine	900	1140	1800	480	850	96.15° ~ 100.87°	79.81° ~ 79.93°
Dongfeng Xiaokang K17	980	1200	1900	420	900	94.39° ~ 97.88°	77.68° ~ 78.51°
Changan Star	910	1210	1850	410	850	81.24° ~ 85.15°	—
Luzun Xiaobawang	950	1250	1850	550	900	90.09° ~ 90.13°	78.58° ~ 81.37°

Usually, in China, when pedestrian's head collides with microbus's engine hood, the impact angle α_2 between

impact direction of pedestrian and engine hood ranges from 77° to 82° , the pedestrian's head injury $HIC > 4684$ and the pedestrian suffers from fatal head injury. In this condition, the head injury of pedestrian can be reduced by increasing the leading edge's height of microbus engine hood H_A .

5 Conclusions

In pedestrian-vehicle collisions, the pedestrian's head has the highest frequency of injury, which often leads to permanent disability or death. Microbuses have been widely used, however, little research has been conducted in the pedestrian head injury related to the microbuses. To overcome the gap, this research investigated the effects of the microbus front structure on the pedestrian head injury.

In this research, according to the geometry and impact dynamics of the pedestrian-microbus collision, mathematic models are developed to describe the pedestrian's collision with the microbus' engine hood and windscreen. Based on the mathematic models developed, the pedestrian head's impact angle α with the engine hood and windscreen are derived. The impact angle α is an important parameter indicating the relationship of pedestrian head injury with the microbus front structure configuration and oblique angles of the engine hood and windscreen.

When the impact angle α is less than 90° , the pedestrian's head injury increases while the impact angle increases. The impact position of head colliding with windshield or engine hood is determined by pedestrian's height and microbus's front size and structure.

When the pedestrian head collides with the microbus engine hood in condition of impact angle $\alpha < 90^\circ$, with the leading edge's height of the engine hood increasing, the impact angle α decreases, and the pedestrian head's injury reduces.

When the pedestrian head collides with microbus windscreen, with the increase of the leading edge's height of the engine hood, the height of the windscreen upper edge, and the engine hood length, the impact angle α increases. However, with the increase of windscreen lower edge height (or the height of engine hood trailing edge) and the length of windscreen, the impact angle α decreases.

Based on the mathematic models and analysis results, simulating experiments are carried-out using LS-Dyna, and a case study of six microbus models of four microbus manufacturers is conducted, which verified the results obtained.

Acknowledgements

The research reported in this paper is supported by the National Natural Science Foundation of China (Grant No. 51108068), the Fundamental Research Funds for the Central Universities (Grant No.2572017DB01), Natural Science Foundation of Heilongjiang province (Grant No. E201350), and the S&T Plan Projects of Heilongjiang Provincial Education Department (Grant No. 11553025).

References

- Chunyu Kong, Jikuang Yang. (2010) 'Logistic regression analysis of pedestrian casualty risk in passenger vehicle collisions in China', *Accident Analysis and Prevention*, Vol. 42, No. 4, pp. 987-993.
- Cheol Oh, Youn-soo Kang, Wonkyu Kim. (2008) 'Assessing the safety benefits of an advanced vehicular technology for protecting pedestrians', *Accident Analysis and Prevention*, Vol. 40, No. 3, pp. 935-942.
- Chu Xiumin, Wan Jian, Yan Xinping, et al. (2008) 'Automobile Safety Technology Based on the Vision of On-board Machines', *China Safety Science Journal*, Vol.18, No. 5, pp. 154-161.
- Cui Yushuo, Zhang Jinhuan, Xu Shucui, et al. (2009) 'A Study on Key Issues of Active Hood and the Conceptual Design of Active Hood Lift System', *Automotive Engineering*, Vol. 31, No. 12, pp. 1120-1122.
- Edwin Ehrlich, Anja Tischer, H. Maxeiner. (2009) 'Lethal pedestrian-Passenger car collisions in Berlin', *Legal Medicine*, Vol. 11, No. 1, pp. 324-326.

- EEVC(2002). 'Improved Test Methods to Evaluate Pedestrian Protection Afforded by Passenger Cars', *European Enhanced Vehicle Safety Committee, Working Group 17*.
- Gianmarco Crocetta, Simone Piantini, Marco Pierini, Ciaran Simms. (2015) 'The influence of vehicle front-end design on pedestrian ground impact', *Accident Analysis and Prevention*, Vol.79, pp. 56–69.
- Liu Kaiyang.(2009) 'Accident Reconstruction and Research on Protection of Pedestrian Head in Vehicle-Pedestrian Collisions'. *Chnagsha: Changsha University of Science & Technology*.
- GB/T 10000-1988. *Human Dimensions of Chinese Adults*. Beijing: STANDARDS PRESS OF CHINA
- H.M. Abdul Aziz, Satish V. Ukkusuri, Samiul Hasan. (2013) 'Exploring the determinants of pedestrian–vehicle crash severity in New York City', *Accident Analysis and Prevention*, Vol. 50, No. 1, pp. 1298-1309.
- Han Yong, YANG Ji-kuang, Koji Mizuno, et al. (2012) 'A study on chest injury mechanism and the effectiveness of a head form impact test for pedestrian chest protection from vehicle collisions', *Safety Science*, Vol. 50, No. 5, pp. 1304-1312.
- Jun Xu, Yibing Li, Guangquan Lu, Wei Zhou. (2009) 'Reconstruction model of vehicle impact speed in pedestrian-vehicle accident', *International Journal of Impact Engineering*, Vol. 36, No. 6, pp. 783-788.
- J.R. Elliott, C.K. Simms, D.P. Wood. (2012) 'Pedestrian head translation, rotation and impact velocity: The influence of vehicle speed, pedestrian speed and pedestrian gait', *Accident Analysis and Prevention*, Vol.45, No.1, pp. 342-353.
- Peng Yong, Chen Yong, Yang Ji-kuang, et al. (2012) 'A study of pedestrian and bicyclist exposure to head injury in passenger car collisions based on accident data and simulations', *Safety Science*, Vol. 50, No. 9, pp. 1749-1759.
- Qiao Weigao, Zhu Xichan. (2006) 'Study of Head Injury and Protection in Vehicle-pedestrian Collisions', *Transaction of the Chinese Society for Agricultural Machinery*, Vol. 37, No. 9, pp.29-31.
- Rikard Fredriksson, Erik Rosén. (2012) 'Integrated pedestrian countermeasures-Potential of head injury reduction combining passive and active countermeasures', *Safety Science*, Vol. 50, No. 3, pp. 400-407.
- Song Xinping, Huang Hu, Shi Runwei. (2009) 'Status and New Technology about Car Pedestrian Protection', *Tractor & Farm Transporter*, Vol. 36, No. 6, pp. 19-22.
- Tetsuo Maki, Janusz Kajzer, Koji Mizuno, et al. (2003) 'Comparative analysis of vehicle-bicyclist and vehicle-pedestrian accidents in Japan', *Accident Analysis and Prevention*, Vol. 35, No. 6, pp. 927-940.
- Yao Jianfeng, Yang Jikuang, Otte Dietmar. (2008) 'Investigation of head injuries by reconstructions of real-world vehicle-versus-adult-pedestrian accidents', *Safety Science*, Vol. 46, No. 7, pp. 1103-1114.
- Xu Hongguo.(2014) 'Qiche Shigu Gongcheng', *Beijing: China Communication Press*.